Environ. Sci. Technol. **2009,** *43,* 4355–4360

Comparative Photoactivity and Antibacterial Properties of C_{60} Fullerenes and Titanium Dioxide Nanoparticles

LÉNA BRUNET,[†] DELINA Y. LYON,[†] ERNEST M. HOTZE,[‡] PEDRO J. J. ALVAREZ,[†] AND MARK R. WIESNER*[,‡]

Department of Civil and Environmental Engineering, Rice University, Houston, Texas, and Department of Civil and Environmental Engineering, Duke University, Durham, North Carolina

Received November 11, 2008. Revised manuscript received March 9, 2009. Accepted March 30, 2009.

The production of reactive oxygen species (ROS) by aqueous suspensions of fullerenes and nano-TiO_2 (Degussa P25) was measured both in ultrapure water and in minimal Davis (MD) microbial growth medium. Fullerol (hydroxylated C_{60}) produced singlet oxygen ($^1O_2$) in ultrapure water and both $^1O_2$ and superoxide ($O_2^{-\bullet}$) in MD medium, but no hydroxyl radicals ($OH^\bullet$) were detected in either case. PVP/C_{60} (C_{60} encapsulated with poly(*N*-vinylpyrrolidone)) was more efficient than fullerol in generating singlet oxygen and superoxide. However, two other aggregates of C_{60}, namely THF/nC_{60} (prepared with tetrahydofuran as transitional solvent) and aqu/nC_{60} (prepared by vigorous stirring of C_{60} powder in water), were not photoactive. Nano-TiO_2 (also present as aggregates) primarily produced hydroxyl radicals in pure water and superoxide in MD medium. Bacterial (*Escherichia coli*) toxicity tests suggest that, unlike nano-TiO_2 which was exclusively phototoxic, the antibacterial activity of fullerene suspensions was linked to ROS production. Nano-TiO_2 may be more efficient for water treatment involving UV or solar energy, to enhance contaminant oxidation and perhaps for disinfection. However, fullerol and PVP/C_{60} may be useful as water treatment agents targeting specific pollutants or microorganisms that are more sensitive to either superoxide or singlet oxygen.

1. Introduction

Photoactive nanomaterials are generally classified into two groups: photosensitizers such as fullerenes, and semiconductors that include metal oxide nanoparticles such as nanoscale titanium oxide (nano-TiO_2). The ability of these nanoparticles to produce reactive oxygen species (ROS), their toxicity (*1*−*3*), and their applicability (*4*−*6*) has received considerable attention. Enhanced photoactivity compared to bulk material or other existing photocatalysts is notably attributable to their small size and large surface area (*7*). Fullerenes also owe their photochemical activity to their strong absorbance throughout the UV/vis spectrum, and to their conjugated molecular structure (*8*).

Distinct mechanisms of ROS generation are displayed by nano-TiO_2 and fullerenes, subsequently leading to differences in ROS speciation. In the case of nano-TiO_2, UV light (<390 nm) induces a separation of charge, generating a hole (h+) in the valence band and an electron in the conduction band (Figure 1A). At the surface of the excited particle, the valence band holes abstract electrons from water and/or hydroxyl ions, generating hydroxyl radicals ($OH^\bullet$). Electrons reduce O_2 to produce the superoxide anion $O_2^{-\bullet}$. Furthermore, $^1O_2$ can be generated by nano-TiO_2, but mostly indirectly via superoxide (*9, 10*). Recombination between h+/e^- pairs also occurs, as well as production of hydroxyl radicals via $O_2^{-\bullet}$. In contrast, electrons in photosensitizers such as fullerenes reach excited singlet ($^1C_{60}$*) and triplet ($^3C_{60}$*) states while staying within the same molecular orbitals (Figure 1B). Due to its longer lifetime, the triplet state ($^3C_{60}$*) is the primary facilitator of energy or electron transfer to oxygen, leading to the formation of $^1O_2$ or $O_2^{-\bullet}$ respectively (*11*). Based on these distinct behaviors, fullerenes and nano-TiO_2 are likely to produce at least three prominent types of ROS ($O_2^{-\bullet}$, $^1O_2$, and $OH^\bullet$), but what is unclear is the relative amount produced by each nanoparticle, and how water chemistry influences these proportions. Such knowledge is of primary interest to compare the oxidative and disinfection power of nano-TiO_2 and fullerenes, which has rarely and only partially been done in the literature (*12*).

Many researchers have reported photocatalytic production of ROS while investigating the mechanism of toxicity of fullerenes and nano-TiO_2. Implications of ROS production include the possibility of lipid peroxidation in membranes, DNA damage due to strand breakage or oxidized nucleotides, and oxidation of amino acids and protein catalytic centers (*13*). The antibacterial and antiviral properties of nano-TiO_2 involve $O_2^{-\bullet}$ and H_2O_2, but especially free and surface-bound $OH^\bullet$ (*14, 15*). The evidence is not so clear for fullerenes. In most studies showing production of ROS or a biological activity linked to light, the fullerenes were either poly hydroxylated (*1, 4, 16, 17*) or encapsulated by a polymer or surfactant (*5, 17*−*19*). Even though some papers reported ROS production and interpret data as indicative of ROS-mediated damage by aggregates like THF/nC_{60} or aqu/nC_{60} (*20*−*23*), these results have been repeatedly called into question and Lyon et al. stressed the need for revisiting these conclusions based on the likely interference of nC_{60} with some fluorescent probes and lipid peroxidation detection methods (*24, 25*). To avoid confusion, a comparison of in vitro nanomaterial effects and ROS generation should be performed using the same solution chemistry (pH, ionic strength, total organic carbon (TOC), etc.), since solutes present in cell culture media may influence the lifetime and the reactivity of the ROS as well as the physicochemical properties of the nanoparticles.

In this work, the role of ROS in possible antibacterial activity associated with several photoactive nanomaterials was investigated in toxicity tests with the model bacterium *Escherichia coli*. Different types of fullerenes (aggregates, hydroxylated, and coated) and nano-TiO_2 (Degussa P25, 80% anatase, 20% rutile) suspensions were evaluated while suspended both in the same microbiological (Minimal Davis) growth medium and in ultrapure water. The oxidative power of each nanoparticle suspension was quantified in terms of concentration and type of ROS produced.

* Corresponding author e-mail: wiesner@duke.edu; phone: (919)-660-5292; fax: (919)-660-5219.
[†] Rice University.
[‡] Duke University.

10.1021/es803093t CCC: $40.75
Published on Web 05/14/2009

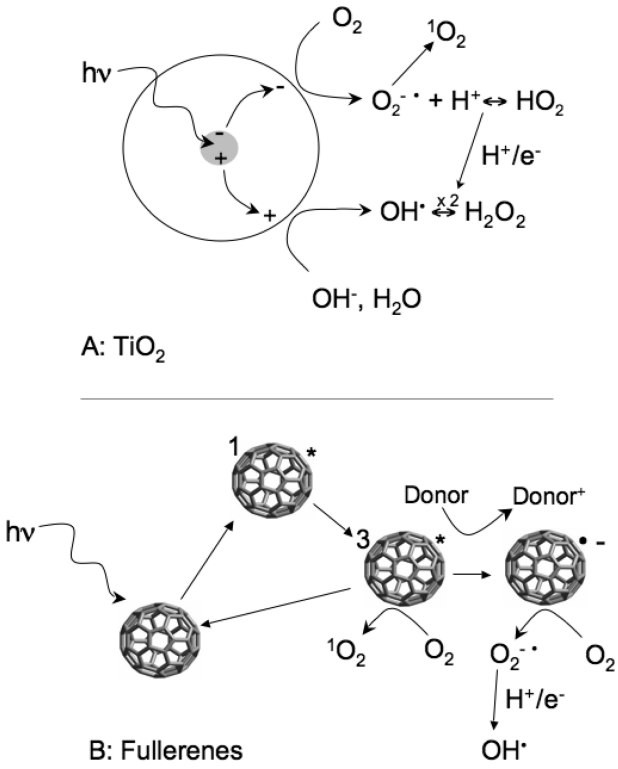

FIGURE 1. Mechanisms of ROS production by nano-TiO_2 (A) and fullerenes (B).

2. Experimental Section

Preparation and Characterization of Nanoparticle Suspensions. Dispersions of fullerenes were prepared from powdered C_{60} (MER, Tucson, AZ). Two varieties of C_{60} aggregates (nC_{60}), referred to as THF/nC_{60} (prepared with tetrahydofuran as transitional solvent), and aqueous nC_{60} (aqu/nC_{60}, prepared by sonicating powdered C_{60} in ultrapure water), as well as PVP/C_{60} (C_{60} encapsulated with poly(*N*-vinylpyrrolidone)), were prepared following the protocols described by Lyon et al. (*26*). Fullerol (hydroxylated C_{60}, $C_{60}(OH)_{24}$) added as a powder as received (MER, Tucson, AZ) to ultrapure water readily forms a stable suspension of aggregates ($nC_{60}(OH)_{24}$). Application of ultrasound was needed to suspend commercial-grade titanium oxide (TiO_2, Aeroxide P25, Degussa, Parsipany NJ) as aggregates in ultrapure water. The suspension was not further filtered, but was sonicated prior to each experiment because of the lack of aggregates size stability over time. Detailed description of these preparation methods and absorption spectra are given in the Supporting Information (SI).

For all suspensions, particle size range was measured using dynamic light scattering (Nanosizer ZS, Malvern Instruments, Worcestershire, UK). The average diameters of THF/nC_{60}, aqu/nC_{60}, PVP/C_{60}, fullerol, and nano-TiO_2 in ultrapure water were 64, 84, 4.4, 122, and 79 nm, respectively (mean value weighted according to the number of particles of each size). The sizes were similar in the minimal Davis (MD) microbial growth medium (pH 7, ionic strength 2.2×10^{-2} M). Detailed characteristics of the nanoparticles including the total amount of carbon measurements and UV absorption spectra are available in the SI.

Irradiation and UV Fluence Measurements. For all experiments measuring ROS production, irradiation was performed with low-pressure UV lamps, in an EMS UV/Cryo chamber (Hatfield, PA) equipped with two 15 W fluorescent ultraviolet bulbs (Philips TLD 15W/08). These bulbs have an output spectrum ranging from 310 to 400 nm, with a peak at 365 nm in the UV-A region. The total irradiance of the UV lamps was 13.6 W/m^2 as measured with a Li-Cor 1800 spectroradiometer. In every experiment, the samples were automatically kept at ~22 °C by the chamber, which would circulate air cooled by dry ice, if necessary.

Assessment of Antibacterial Activity. *E. coli* K12 (ATCC 25404) was used as a model bacterium to assess the antibacterial activity of various nanoparticle suspensions in minimal Davis Medium (MD) with the following composition: 0.7 g of K_2HPO_4, 0.2 g of KH_2PO_4, 1 g of $(NH_4)_2SO_4$, 0.5 g of sodium citrate, 0.1 g of $MgSO_4 \cdot 7\,H_2O$, and 1 g of glucose, pH 7. To assess the number of colony forming units (CFU) that survived nanomaterial exposure, an overnight culture of *E. coli* K12 was diluted into MD with no glucose to about 10^3 CFU/mL. The nanomaterials were added to cells at a final concentration of 140 μM, and the samples were incubated in the dark or under the illumination of a 40 W incandescent white lamp for 6 h. The cells were diluted 10-fold, prior to plating 50 μL onto LB agar plates. The plates were incubated overnight at 37 °C, and the colonies were counted. The results are presented as the percent of surviving bacteria, calculated by dividing the number of colonies on the sample plate by the number of colonies on a control plate (no nanomaterials) incubated under the same conditions.

Detection of Superoxide by XTT Reduction. XTT (2,3-bis(2-methoxy-4-nitro-5-sulfophenyl)-2H-tetrazolium-5-carboxanilide) is a widely used superoxide probe that offers the advantage of being specific, water-soluble, and resistant to auto-oxidation (*27, 28*). XTT reduction by $O_2^{\bullet-}$ results in the formation of XTT-formazan. The formazan produced has an absorption peak at 470 nm that can be used to quantify the relative amount of superoxide present (*16, 27, 28*). Samples were prepared by mixing 5 μM nanoparticles and 100 μM XTT in 10 mL flasks and then exposing them to the aforementioned UV source for 30 h. The experiments were conducted in either nonbuffered ultrapure water or in MD medium. Color change was measured by absorbance at 470 nm using an Ultrospec 2100 pro UV/Visible spectrophotometer (Amersham Biosciences, Pittsburgh, PA).

Detection of Singlet Oxygen with SOSG. The singlet oxygen sensor green reagent (SOSG, Molecular Probes-Invitrogen, Carlsbad, CA), is a dye-quencher pairing that emits green fluorescence in the presence of $^1O_2$, with excitation and emission peaks at 504 and 525 nm, respectively. A stock solution of SOSG (5 mM) was prepared by dissolution in methanol and then dilution in water. The samples containing 25 μM nanoparticles, 1.3 μM SOSG, and, if applicable, MD medium, were exposed to UV for less than 3 h. At different time intervals, a volume of 0.5 mL was collected and mixed with 0.3 mL of water or 0.3 mL of NaN_3 (100 mM), known to be a specific quencher for $^1O_2$. Fluorescence emissions at 528 nm of the quenched and the diluted samples were measured with a fluorescence spectrophotometer (Hitachi F2500, Tokyo, Japan) using an excitation wavelength of 480 nm.

Detection of Hydroxyl Radicals with pCBA. Para-chlorobenzoic acid (pCBA) is a well-known probe used to detect hydroxyl radicals in water systems (*15, 29, 30*). The degradation of pCBA by strong oxidative radicals was monitored by high-pressure liquid chromatography (Waters 2695 Separations Module, Waters, Milford, MA). Ten mL solutions containing 20 μM nanoparticles and 25 μM pCBA were exposed to UV for 9 h. To remove nanoparticles from the solution prior to the HPLC analysis, sampled solutions were filtered with 0.02 μm Anopore syringe filters (Anotop 10, Whatman, Florham Park, NJ). A C_{18} reverse-phase column (Nova-Pak C_{18}, Waters, 3.9 mm by 150 mm) was used with a UV detector (Waters 996 Photodiode Array Detector, Waters, Milford, MA) at a wavelength of 232 nm to measure the concentration of pCBA. A solvent mixture of 50% water/50%

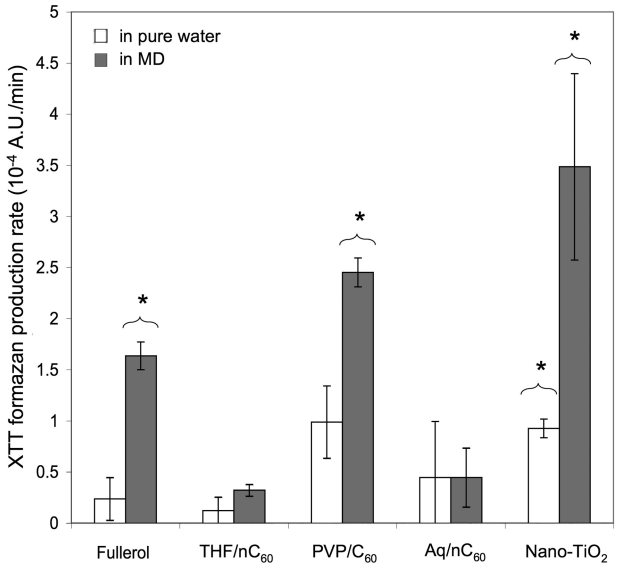

FIGURE 2. Superoxide production by different nanoparticle suspensions (5 μM each) exposed to UV in ultrapure water or in MD. Generation of $O_2^{-\bullet}$ was assessed per XTT-formazan production, measured as increase in absorbance at 470 nm. Bars indicate the standard deviation from the mean ($n = 3$). * denotes a significant difference from the control at the 95% confidence level.

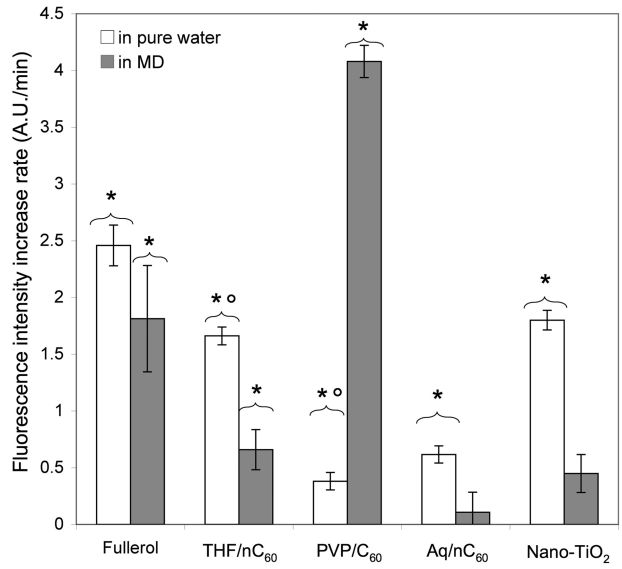

FIGURE 3. Differences in singlet oxygen production by different nanoparticle suspensions (25 μM each) exposed to UV in ultrapure water or in MD. Generation of $O_2^{-\bullet}$ was assessed per SOSG fluorescence. Bars indicate the standard deviation of the mean ($n = 3$). * denotes a significant difference from the control at the 95% confidence level. THF/nC_{60} and PVP/C_{60} induced a drop in pH (pH ~4) that deactivated the SOSG dye.

acetonitrile was employed as the mobile phase in isocratic mode with a flow of 0.4 mL/min. The experiment was carried out in ultrapure water or in MD medium.

All the experiments were performed in triplicate. Statistically significant results were determined with the student *t* test at the 95% confidence level.

3. Results and Discussion

MD Medium Enables Superoxide Production by Nano-TiO_2, Fullerol, and PVP/C_{60}. In ultrapure water, only nano-TiO_2 produced small but significant amounts of superoxide (Figure 2). Superoxide production rates were negligible for the fullerenes. On the other hand, superoxide production was significantly higher in MD medium for suspensions of nano-TiO_2, fullerol, and PVP/C_{60}. These results illustrate different ROS production mechanisms for fullerenes and nano-TiO_2. To validate these assays, control tests showed that superoxide dismutase (SOD) completely suppressed XTT formazan production in both media (data not shown). Another experiment showed that the PVP solution in the absence of C_{60} was photoinert (data not shown). However, one possibility that remains to be verified is whether or not the polymer PVP itself, with its nitrogen and oxygen atoms, can supply the photoexcited triplet $^3C_{60}$* with electrons.

In MD medium, nano-TiO_2 generated the most $O_2^{-\bullet}$, followed by PVP/C_{60}, and then fullerol. The two fullerenes released, respectively, 70% and 47% of the amount of superoxide produced by nano-TiO_2. High pH values may play a role in increasing photoactivity. In the case of nano-TiO_2, superoxide production is enhanced at neutral and basic pH values that are more favorable to ROS formation through charge effects at the surface of nano-TiO_2 (*31*) while electron donors reduce the recombination of photoexcited electron−hole pairs (*32*). Also, hydroxyl and carboxylate groups on glucose (1 g/L) and citrate (0.5 g/L), respectively, may be pH-sensitive electron donors. The exact role of pH in the mechanism of superoxide generation by fullerenes is unclear and the specific effects of electron donors and water chemistry on ROS generation is an active area of research. Photoactive fullerenes are known to mediate electron transfer from the electron donor (e.g., glucose and/or Na-citrate) by forming the anion $^3C_{60}$* (*16*). THF/nC_{60} and aqu/nC_{60} are ineffective in producing ROS due to their structure (*16, 18*).

Fullerol and PVP/C_{60} Favor Singlet Oxygen Production. The production of $^1O_2$ is depicted as the rate of increase in fluorescence intensity from SOSG, corrected for the medium's fluorescence (Figure 3). More details about the SOSG dye and the control tests performed are available in the SI. In ultrapure water, the pH was not controlled; consequently, fullerol, aqu/nC_{60}, and nano-TiO_2 had pH values around 5.5−6, while PVP/C_{60} and THF/nC_{60} exhibited more acidic pH around 4 which deactivates the SOGS dye (information obtained from Molecular Probes-Invitrogen). Under these conditions, fullerol displayed the highest ROS production under UV irradiation, followed by nano-TiO_2. Aqu/nC_{60} appeared to produce small amounts of singlet oxygen. However, these results are in contrast with previous reports where singlet oxygen production by aq/nC_{60} was not detected (*16*) raising the possibility that the SOSG produces a false positive when compared with the more reliable method of detection by electron paramagnetic resonance. Similarly, THF/nC_{60} apparently induced a reaction from the dye, but the low pH prevents any conclusions about relative $^1O_2$ production capacity from being drawn. The drop in pH also accounts for the lack of fluorescence in presence of PVP/C_{60}.

In MD medium buffered at pH 7, fullerol and especially PVP/C_{60} induced a substantial increase in fluorescence compared to the MD medium alone, indicating efficient $^1O_2$ production. It was verified that PVP solution in the absence of C_{60} did not show singlet oxygen production under identical conditions (data not shown). In contrast, nano-TiO_2 did not generate significant amounts of $^1O_2$, and aqu/nC_{60} was photoinert regarding SOSG. Two interpretations can account for the reduced production of singlet oxygen by nano-TiO_2 in MD compared to pure water, based on the conversion of superoxide into singlet oxygen (*9, 33*): (1) the electron transfer between $OH^\bullet$ and $O_2^{-\bullet}$ ($OH^\bullet + O_2^{-\bullet} \rightarrow {}^1O_2 + OH^-$) is less likely to occur in MD as $OH^\bullet$ radicals are quenched by Na-citrate

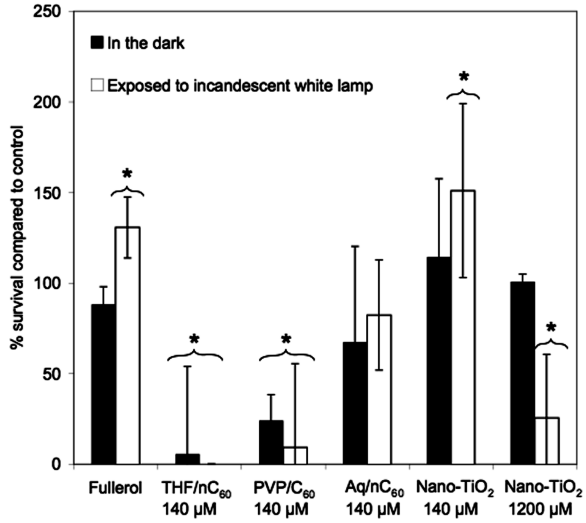

FIGURE 4. Percent survival of *E. coli* exposed to nanomaterials ($n = 6$). * denotes a significant difference from the control at the 95% confidence level. The control was performed without nanoparticles, in the dark or exposed to an incandescent white lamp.

and/or glucose; and (2) conversion also occurs more in acidic pH ($2\ H^+ + 2\ O_2^{-\bullet} \rightarrow {}^1O_2 + H_2O_2$). It is unlikely that a compound from the MD medium could have quenched singlet oxygen since this effect was not observed with the other nanoparticles. THF/nC_{60} generated a small amount of $^1O_2$. However, given the lack of superoxide production by THF/nC_{60} in experiments with XTT, it is more likely that THF/nC_{60} interfered with the SOSG dye. Such an interference of THF/nC_{60} has been reported with other fluorescent probes (*24, 27*). Taken together, these data show that, consistent with the results obtained with superoxide production, singlet oxygen was efficiently produced by fullerol and PVP/C_{60}.

Nano-TiO_2 Produces Hydroxyl Radicals; C_{60} Fullerene and Fullerol Do Not. Nano-TiO_2 generated significant amounts of $OH^\bullet$ when irradiated by UV in ultrapure water (47% of pCBA degradation after 9 h of UV-A exposure). This result was expected as nano-TiO_2 is mostly studied for its photocatalytic production of hydroxyl radicals. In contrast, none of the fullerenes (up to 20 μM) generate hydroxyl radicals. Interestingly, hydroxyl radical generation by nano-TiO_2 was inhibited in the MD medium, with or without glucose. Consistent with superoxide enhancement production, this can be rationalized by the nonspecific reaction of $OH^\bullet$ radicals with many organic and some inorganic species (*34*). In this case, $OH^\bullet$ radicals may have reacted with Na-citrate and/or glucose.

Fullerenes Display Different Degrees of Antibacterial Activity Regardless of Light; Only Nano-TiO_2 is Exclusively Phototoxic. The nanomaterials were assessed for antibacterial effects by exposing them to *E. coli* for 6 h under a white incandescent light or in the dark. Bacterial survival was monitored by the number of colony forming units in bacterial suspensions exposed to 140 μM of nanoparticles as compared to a control. As shown in Figure 4, fullerol and aqu/nC_{60} did not exert significant antibacterial activity regardless of light exposure. On the contrary, the presence of fullerol seems to encourage the growth of colonies under light. The heat from the lamp or the roughness of the surface could account for such a result. A similar effect was observed for biofilm formation with THF/nC_{60} coatings by Lyon et al., with the hypothesis that nanoparticle coatings provide increased surface area with a rougher and more hydrophobic surface (*35*).

While the lack of toxicity of fullerol confirms the results obtained in earlier studies (*2, 36*), the absence of antimicrobial activity of aqu/nC_{60} appears to contradict our previous results (*26*). The aqu/nC_{60} used in this experiment was sonicated which may have altered its biological impact. Further research needs to be performed to elucidate the actual role of sonication on the structure, surface, and subsequent biological and physicochemical properties of fullerenes aggregates. The other fullerene-based materials have significant antibacterial properties even in the dark. While the THF/nC_{60} appeared to vary in toxicity according to the presence of light, these differences are not statistically significant at the 95% confidence interval. PVP/C_{60} is significantly more potent under light than in the dark, but still retained some activity in the dark. Nano-TiO_2 did not exert toxicity at a concentration of 140 μM (~11 ppm). As with fullerol, growth was enhanced when low concentrations of nano-TiO_2 and cells were exposed to light. In the literature, the concentration of nano-TiO_2 usually required to kill bacteria varies between 10^{-3} and 5000 ppm (*37*) (*38*), according to the size of the particles and the intensity and wavelength of the light used. In our study, at 100 ppm (~1200 μM), nano-TiO_2 was phototoxic with 25% of the exposed bacteria surviving whereas no impact was observed in the dark.

ROS Speciation. We examined ROS production in ultrapure water and in MD medium using specific detection methods for superoxide, singlet oxygen, and hydroxyl radicals. To compare the relative amount of each type of ROS, SOSG fluorescence, XTT, and pCBA absorbances were converted to singlet oxygen, superoxide, and hydroxyl radical concentrations, respectively, after application of calibration curves. Table 1 summarizes the ROS generation rates, normalized by the concentration of nanoparticles. It is clear that fullerol and PVP/C_{60} were able to produce $^1O_2$ and $O_2^{-\bullet}$, while THF/nC_{60} and aqu/nC_{60} were not photoactive. However, superoxide production was linked to the presence of electron donors in MD and no hydroxyl radicals production was detected, which negates the idea that fullerenes could produce hydroxyl radicals via superoxide (*19*), at least not without an electron donor. In contrast, nano-TiO_2 was able to produce ROS in pure water and large amounts of superoxide in MD medium. Globally, the sum production of $^1O_2$, $O_2^{-\bullet}$, and $OH^\bullet$ for PVP/C_{60} and fullerol in MD were similar to total ROS produced by nano-TiO_2 (Table 1).

Biological Implications of Nano-TiO_2 and Fullerenes Photoactivity. Comparing toxicity results and ROS production in MD medium confirms that nano-TiO_2 primarily owes it toxicity to its photochemical properties (mainly superoxide, as hydroxyl radicals were quenched in MD). In contrast, for fullerenes, it was observed that (1) THF/nC_{60} exhibits a strong toxicity regardless of light while no significant amount of ROS was detected; (2) aqu/nC_{60} is also photochemically inert and less harmful to bacteria; (3) fullerol produces ROS (~0.29 μM/h/μM total) but not in sufficient quantities to exert a significant antibacterial effect; and (4) PVP/C_{60} toxicity under a incandescent white lamp light probably does not correlate to its ROS production (~0.50 μM/h/μM) since toxicity still occurs in the dark. Overall, our approach demonstrates that there is no correlation between the ROS production of fullerenes and antibacterial activity; ergo, fullerene antibacterial activity, unlike nano-TiO_2, is not solely due to ROS. This conclusion is consistent with the recent results obtained by Lyon et al. who propose that THF/nC_{60} exerts direct protein oxidation in the cell membrane, causing change in cell membrane potential and interruption of cellular respiration (*25*).

Potential Applications of Fullerenes and Nano-TiO_2. Photoactive nanomaterials have a wide range of applications. Water purification systems based on nano-TiO_2 photoca-

TABLE 1. Summary of the ROS Generation by Nanoparticles in Ultra-Pure Water and in MD Medium

nanoparticles	fullerol		PVP/C_{60}		THF/nC_{60}		aqu/nC_{60}		nano-TiO_2	
medium	ultrapure water	MD medium	ultrapure water	MD medium	ultrapure water	MD medium	ultrapure water	MD medium	ultrapure water	MD medium
[$^1O_2$], μM/h/μM	0.12	0.09	[b]	**0.20**	[b]	0.03	0.03	[a]	0.09	[a]
[$O_2^{-\bullet}$], μM/h/μM	[a]	**0.20**	[a]	**0.30**	[a]	[a]	[a]	[a]	0.12	0.43
[$OH^\bullet$], μM/h/μM	[a]	[a]	[a]	[a]	[a]	[a]	[a]	[a]	0.13	[a]

[a] Indicates ROS were not detected or not statistically significant. [b] No conclusion was drawn from this test as the very low pH deactivated the probe.

talysis already exist (e.g., Purifics). Fullerenes are not yet commercially exploited for their photosensitivity, but both nanomaterials offer promises for advanced oxidation processes in water treatment (*6, 39*), medical applications like photodynamic therapy (*40, 41*) or solar cells (*42, 43*). Both display antibacterial (*14, 26*) and antiviral properties (*4, 15*) and are therefore proposed to enhance UV and solar disinfection (*37, 39*), or produce biofouling-resistant filtration membranes (*44*).

Singlet oxygen is a selective oxidant with a short lifetime (3.8 μs in pure water) (*45*). A rapid deactivation will induce even shorter lifetimes in biological systems or in natural waters. It is presumed to be the most reactive species in photodynamic therapy (PDT) (*46*). Addition of dyes with high yields of $^1O_2$ has also been suggested to oxidize organic compounds and some bacteria for wastewater treatment (*47*). But Haag et al. concluded that the concentrations found in natural waters would be sufficient for only a few types of micropollutants (*48*). Hydroxyl radicals are strong and nonselective ROS with a lifetime of approximately 10 μs in natural waters (*49*). They can induce similar damage as traditional photosensitizers, but might be too harmful for biomedical applications. On the other hand, applications requiring a strong oxidant for a complete inactivation of microorganisms or degradation of organic pollutants might be better served by nanoparticles that produce hydroxyl radicals. Finally, superoxide is quite toxic biologically and can act as a reducer or an oxidant (*50*).

The above considerations imply that the efficient $^1O_2$ generation by hydroxylated and polymer-coated fullerenes makes them better candidates than nano-TiO_2 for applications in photodynamic therapy and for medical applications in general. In contrast, fullerenes and derivatives may not, a priori, do a better job than nano-TiO_2 for disinfection by UV or advanced oxidation processes in water treatment applications, based on $OH^\bullet$ radical production. However, this statement can be mitigated by the specific degradation of some compounds or microorganisms by only a certain type of ROS. Epe et al. gave evidence that DNA damage observed in *Salmonella* cells was emanating from the direct action of $^1O_2$ whereas $O_2^{-\bullet}$ or $OH^\bullet$ would not contribute much (*51*). Badireddy et al. also observed inactivation of MS-2 bacteriophage by fullerol due to singlet oxygen and superoxide (*4*). Unpublished results demonstrated that, in that latter case, nano-TiO_2 was not efficient. Additionally, some pollutants that cannot be classically degraded by hydroxyl radicals will be reduced by superoxide instead. As an example, Choi et al. proposed to exploit nano-TiO_2's capability to generate superoxide, doped in the presence of electron donors, for photoreductive degradation of halogenated hydrocarbons (*32*). Considering the relatively high yields of superoxide production by fullerol and PVP/C_{60}, such applications could also be considered for fullerenes.

Based on these findings, nano-TiO_2 is expected to be a more efficient nanomaterial for environmental oxidation, and perhaps enhancing UV disinfection applications, although photoactive fullerenes might be efficient complementary tools for specific targets.

Acknowledgments

This work was funded by the National Science Foundation (NSF) grant BES-0508207 and the EPA STAR program (91650901-0).

Supporting Information Available

Preparation and characterization techniques of fullerenes and nano-TiO_2, including Total Carbon Analysis measurements and UV absorption spectra; complementary information about the probe SOSG, notably the control tests performed to validate its functioning. This material is available free of charge via the Internet at http://pubs.acs.org.

Literature Cited

(1) 7.4Pickering, K. D.; Wiesner, M. R. Fullerol-sensitized production of reactive oxygen species in aqueous solution. *Environ. Sci. Technol.* **2005**, *39* (5), 1359–1365.
(2) 7.4Lyon, D. Y.; Fortner, J. D.; Sayes, C. M.; Colvin, V. L.; Hughes, J. B. Bacterial cell association and antimicrobial activity of a C-60 water suspension. *Environ. Toxicol. Chem.* **2005**, *24* (11), 2757–2762.
(3) 7.4Long, T. C.; Saleh, N.; Tilton, R. D.; Lowry, G. V.; Veronesi, B. Titanium dioxide (p25) produces reactive oxygen species in immortalized brain microglia (bv2): Implications for nanoparticle neurotoxicity. *Environ. Sci. Technol.* **2006**, *40* (14), 4346–4352.
(4) 7.4Badireddy, A. R.; Hotze, E. M.; Chellam, S.; Alvarez, P.; Wiesner, M. R. Inactivation of bacteriophages via photosensitization of fullerol nanoparticles. *Environ. Sci. Technol.* **2007**, *41*, 6627–6632.
(5) 7.4Kai, Y.; Komazawa, Y.; Miyajima, A.; Miyata, N.; Yamakoshi, Y. [60]Fullerene as a novel photoinduced antibiotic. *Fullerenes, Nanotubes, Carbon Nanostruct.* **2003**, *11* (1), 79–87.
(6) 7.4Bauer, R.; Waldner, G.; Fallmann, H.; Hager, S.; Klare, M.; Krutzler, T. The photo-Fenton reaction and the TiO_2/UV process for waste water treatment-novel developments. *Catal. Today* **1999**, *53*, 131–144.
(7) 7.4Nel, A.; Xia, T.; Madler, L.; Li, N. Toxic potential of materials at the nanolevel. *Science* **2006**, *311* (5761), 622–627.
(8) 7.4Ausman, K. D.; Weisman, R. B. Kinetics of fullerene triplet states. *Res. Chem. Intermed.* **1997**, *23*, 431–451.
(9) 7.4Daimon, T.; Nosaka, Y. Formation and behavior of singlet oxygen in TiO_2 photocatalysis studied by detection of near-infrared phosphorescence. *J. Phys. Chem.* **2007**, *111*, 4420–4424.
(10) 7.4Hirakawa, K.; Hirano, T. Singlet oxygen generation photocatalyzed by TiO_2 particles and its contribution to biomolecule damage. *Chem. Lett.* **2006**, *35* (8), 832–833.
(11) 7.4Arbogast, J. W.; Darmanyan, A. P.; Foote, C. S.; Rubin, Y.; Diedrich, F. N.; Alvarez, M. M.; Anz, S. J.; Whetten, R. L. Photophysical properties of C_{60}. *J. Phys. Chem.* **1991**, *95*, 11.
(12) 7.4Xia, T.; Kovochich, M.; Brant, J.; Hotze, E. M.; Sempf, J.; Oberley, T.; Sioutas, C.; Yeh, J. I.; Wiesner, M. R.; Nel, A. Comparison of the abilities of ambient and manufactured nanoparticles to induce cellular toxicity according to an oxidative stress paradigm. *Nano Lett.* **2006**, *6* (8), 1794–1807.
(13) 7.4Cabiscol, E.; Tamarit, J.; Ros, J. Oxidative stress in bacteria and protein damage by reactive oxygen species. *Int. Microbiol.* **2000**, *3*, 3–8.

(14) 7.4Maness, P.-C.; Smolinski, S.; Blake, D. M.; Huang, Z.; Wolfrum, E. J.; Jacoby, W. A. Bactericidal activity of photocatalytic TiO_2 reaction: Toward an understanding of its killing mechanism. *Appl. Environ. Microbiol.* **1999**, *65* (9), 4094–4098.
(15) 7.4Cho, M.; Chung, H.; Choi, W.; Yoon, J. Different inactivation behavior of MS-2 phage and *Escherichia coli* in TiO_2 photocatalytic disinfection. *Appl. Environ. Microbiol.* **2005**, *71* (1), 270–275.
(16) 7.4Hotze, E. M.; Labille, J.; Alvarez, P.; Wiesner, M. R. Mechanisms of photochemistry and reactive oxygen production by fullerene suspensions in water. *Environ. Sci. Technol.* **2008**, *42* (11), 4175–4180.
(17) 7.4Guldi, D. M.; Asmus, K. D. Activity of water-soluble fullerenes towards (OH)-o-center dot-radicals and molecular oxygen. *Radiat. Phys. Chem.* **1999**, *56* (4), 449–456.
(18) 7.4Lee, J.; Fortner, J. D.; Hugues, J. B.; Kim, J.-H. Photochemical production of reactive oxygen species by C_{60} in the aqueous phase during UV irradiation. *Environ. Sci. Technol.* **2007**, *41* (7), 2529–2535.
(19) 7.4Yamakoshi, Y.; Umezawa, N.; Ryu, A.; Arakane, K.; Miyata, N.; Goda, Y.; Masumizu, T.; Nagano, T. Active oxygen species generated from photoexcited fullerene (C-60) as potential medicines: $O_2^{-\cdot}$ versus $^1O_2$. *J. Am. Chem. Soc.* **2003**, *125* (42), 12803–12809.
(20) 7.4Sayes, C. M.; Gobin, A. M.; Ausman, K. D.; Mendez, J.; West, J. L.; Colvin, V. L. Nano-C-60 cytotoxicity is due to lipid peroxidation. *Biomaterials* **2005**, *26* (36), 7587–7595.
(21) 7.4Isakovic, A.; Markovic, Z.; Todorovic-Markovic, B.; Nikolic, N.; Vranjes-Djuric, S.; Mirkovic, M.; Dramicanin, M.; Harhaji, L.; Raicevic, N.; Nikolic, Z.; Trajkovic, V. Distinct cytotoxic mechanisms of pristine versus hydroxylated fullerene. *Toxicol. Sci.* **2006**, *91* (1), 173–183.
(22) 7.4Markovic, Z.; Todorovic-Markovic, B.; Kleut, D.; Nikolic, N.; Vranjes-Djuric, S.; Misirkic, M.; Vucicevic, L.; Janjetovic, K.; Isakovic, A.; Harhaji, L.; Babic-Stojic, B.; Dramicanin, M.; Trajkovic, V. The mechanism of cell-damaging reactive oxygen generation of colloidal fullerenes. *Biomaterials* **2007**, *28* (36), 5437–5448.
(23) 7.4Oberdoster, E. Manufactured nanomaterials (fullerenes, C_{60}) induce oxidative stress in the brain of juvenile largemouth brass. *Environ. Health Perspect.* **2004**, *112* (10), 1058.
(24) 7.4Lyon, D. Y.; Brunet, L.; Hinkal, G. W.; Wiesner, M. R.; Alvarez, P. J. J. Antibacterial activity of fullerene water suspension (nC_{60}) is not due to ROS-mediated damage. *Nano Lett.* **2008**, *8* (5), 1539–1549.
(25) 7.4Lyon, D. Y.; Alvarez, P. J. J. Fullerene water suspension (nC_{60}) exerts antibacterial effects via ROS-independent protein oxidation. *Environ. Sci. Technol.* **2008**, *42* (21), 8127–8132.
(26) 7.4Lyon, D. Y.; Adams, L. K.; Falkner, J. C.; Alvarez, P. J. J. Antibacterial activity of fullerene water suspensions: Effects of preparation method and particle size. *Environ, Sci, Technol,* **2006**, *40* (14), 4360–4366.
(27) 7.4Bartosz, G. Use of spectroscopic probes for detection of reactive oxygen species. *Clin. Chim. Acta* **2006**, *368*, 53–76.
(28) 7.4Ukeda, H.; Maeda, S.; Ishili, T.; Sawamura, M. Spectrophotometric assay for superoxide dismutase based on tetrazolium salt 3′-1-(phenylamino)-carbonyl-3,4-tetrazolium]-bis(4-methoxy-6-nitro)benzenesulfonic acid hydate reduction by xanthine-xanthine oxidase. *Anal. Biochem.* **1997**, *251*, 206–209.
(29) 7.4Pi, Y.; Schumacher, J.; Jekel, M. The use of para-chlorobenzoic acid (pcba) as an ozone/hydroxyla radical compound. *Ozone Sci. Eng.* **2005**, *27*, 431–436.
(30) 7.4Elovitz, M. S.; von Gunten, U. Hydroxyl radical/ozone ratios during ozonation processes. I. The RCT concept. *Ozone Sci. Eng.* **1999**, *21* (3), 239–260.
(31) 7.4Kormann, C.; Bahnemann, D. W.; Hoffmann, M. R. Photolysis of chloroform and other organic molecules in aqueous TiO_2 suspensions. *Environ. Sci. Technol.* **1991**, *25*, 454–500.
(32) Choi, W.; Hoffmann, M. R. Photoreductive mechanism of cC_{l4} degragation on TiO_2 particles and effects of electron donors. *Environ. Sci. Technol.* **1995**, *29*, 1646–1654.
(33) 7.4Khan, A. U.; Kasha, M. Singlet molecular oxygen in the Haber-Weiss reaction. *Proc. Natl. Acad. Sci. U.S.A.* **1994**, *91*, 12365–12367.
(34) 7.4Haag, W. R.; Yao, C. C. D. Rate constants for reaction of hydroxyl radicals with several drinking water contaminants. *Environ. Sci. Technol.* **1992**, *26* (5), 1005–1013.
(35) 7.4Lyon, D. Y.; Brown, D.; Sundstrom, E. R.; Alvarez, P. J. J. Assessing the antibiofouling potential of a fullerene-coated surface. *Int. Biodegradation Biodeterioration* **2008**, *62* (4), 475–478.
(36) 7.4Sayes, C. M.; Fortner, J. D.; Guo, W.; Lyon, D.; Boyd, A. M.; Ausman, K. C.; Tao, Y. J.; Sitharaman, B.; Wilson, L. J.; Hughes, J. B.; West, J. L.; Colvin, V. L. The differential cytotoxicity of water-soluble fullerenes. *Nano Lett.* **2004**, *4* (10), 1881–1887.
(37) 7.4Matsunaga, T.; Okochi, M. TiO_2-mediated photochemical disinfection of *Escherichia coli* using optical fibers. *Environ. Sci. Technol.* **1995**, *29*, 501–505.
(38) 7.4Adams, L. K.; Lyon, D. Y.; McIntosh, A.; Alvarez, P. J. J. Comparative toxicity of nano-scale TiO_2, SiO_2 and ZNO water suspensions. *Water Sci. Technol.* **2006**, *54*, 11–12.
(39) 7.4Bottero, J. Y.; Rose, J.; Wiesner, M. R. Nanotechnologies: Tools for sustainability in a new wave of water treatment processes. *Int. Environ. Assess. Manage.* **2006**, *2* (4), 391–395.
(40) 7.4Wang, S.; Gao, R.; Zhou, F.; Selke, M. Nanomaterials and singlet oxygen photosensitizers: Potential applications in photodynamic therapy. *J. Mater. Chem.* **2004**, *14*, 487–493.
(41) 7.4Zarubaev, V. V.; Belousiva, I. M.; Kiselev, O. I.; Piotrovski, L. B.; Anfimov, P. M.; Krisko, T. C.; Muraviova, T. D.; Rylkov, V. V.; Starodubzev, A. M.; Sirotkin, A. C. Photodynamic inactivation of influenza virus with fullerene C_{60} suspension in allantoic fluid. *Photodiagnosis Photodynamic Therapy* **2007**, *4* (1), 31–35.
(42) 7.4Brabec, C. J.; Sariciftci, N. S.; Hummelen, J. C. Plastic solar cells. *Adv. Funct. Mater.* **2001**, *11* (1), 15–26.
(43) 7.4Ni, M.; Leung, M. K. H.; Leung, D. Y. C.; Sumathy, K. A review and recent developments in photocatalytic water-splitting using TiO_2 for hydrogen production. *Renewable Sustainable Energy Rev.* **2005**, *11* (3), 401–425.
(44) 7.4Kim, S. H.; Kwak, S. Y.; Sohn, B. H.; Park, T. H. Design of TiO_2 nanoparticle self-assembled aromatic polyamide thin-film-composite (TFC) membrane as an approach to solve biofouling problem. *J. Membr. Sci.* **2003**, *211*, 157–165.
(45) 7.4Foote, C. S.; Valentine, J. S.; Liebman, J. F. *Active Oxygen in Chemistry*; Blackie Academic & Professional: Glasgow, 1995.
(46) 7.4Weishaupt, K. R.; Gomer, C. J.; Dougherty, T. J. Identification of singlet oxygen as the cytotoxic agent in photo-inactivation of a murine tumor. *Cancer Res.* **1976**, *36*, 2326–2329.
(47) 7.4Acher, A. J.; Rosenthal, I. Dye-sensitized photo-oxidation - a new approach to the treatment of organic matter in sewage effluents. *Water Res.* **1977**, *11*, 557–562.
(48) 7.4Haag, W. R.; Hoigne, J. Singlet oxygen in surface waters. 3. Photochemical formation and steady-state concentrations in various types of waters. *Environ. Sci. Technol.* **1986**, *20*, 341–348.
(49) 7.4Hoigne, J. Inter-calibration of OH radical sources and water quality parameters. *Water Sci. Technol.* **1997**, *35*, 4.
(50) 7.4Fridovich, I. Biological effects of the superoxide radical. *Arch. Biochem. Biophys.* **1986**, *247* (1), 1–11.
(51) 7.4Epe, B.; Hegler, J.; Wild, D. Singlet oxygen as an ultimately reactive species in *Salmonella typhimurium* DNA damage induced by methylene blue/visible light. *Carcinogenesis* **1989**, *10* (11), 2019–2024.

ES803093T